Low dispersity polymers in *ab initio* emulsion polymerization: Improved macroRAFT agent performance in heterogeneous media

Robert A. E. Richardson,[1a] Thiago R. Guimarães,[2b] Murtaza Khan,[2c] Graeme Moad,[3d] Per B. Zetterlund[2e]* and Sébastien Perrier[1,4,5f]*

[1] Department of Chemistry, University of Warwick, Coventry, CV4 7AL, UK.

[2] Centre for Advanced Macromolecular Design (CAMD), School of Chemical Engineering, The University of New South Wales, Sydney, NSW, 2052, Australia.

[3] CSIRO Manufacturing, Bag 10, Clayton South, VIC 3169, Australia.

[4] Faculty of Pharmacy and Pharmaceutical Sciences, Monash University, 381 Royal Parade, Parkville, VIC 3052, Australia

[5] Warwick Medical School, University of Warwick, Coventry, CV4 7AL, UK

[a] R.A.E.Richardson@warwick.ac.uk
[b] thiago.guimarois@gmail.com
[c]
[d] graeme.moad@csiro.au
[e] p.zetterlund@unsw.edu.au
[f] S.Perrier@warwick.ac.uk

Abstract

We demonstrate that the in-built monomer feeding mechanism in an emulsion polymerization can be used to dramatically increase control (providing low molar mass dispersity ($Đ$) ≤ 1.15) over polymerizations mediated by RAFT agents with relatively low transfer constants (C_{tr}). An amphiphilic RAFT agent [RSC(=S)Z], based on a hydrophilic methacrylic R group [$\dot{\mathbf{C}}(CH_3)_2CO_2$-PEG] and hydrophobic Z group with $C_{tr} \approx 11$, was used to mediate the polymerization of a range of methacrylate monomers under both heterogeneous and homogeneous conditions. Consistent with the low C_{tr}, batch miniemulsion or solution polymerizations did not provide polymers with low $Đ$, an expected behaviour attributable to the low chain transfer constant of the RAFT agent. The issue of a low C_{tr} is overcome in an emulsion polymerization when the [monomer]/[RAFT agent] ratio at the locus of polymerization is substantially lower than the overall ratio, due to the presence of a discrete monomer droplet phase. The proposed mechanism is supported by a theoretical model. As a demonstration of the increased level of control achievable, the system has been exploited to generate methacrylate multiblock copolymers.

Introduction

Well-defined polymers are ubiquitous within biological systems, serving a range of functions from catalysis, in the case of enzymes, to providing the structural support of chitosan exoskeletons.[1-3] In the majority of cases the monomer sequence in these biopolymers are finely controlled. Attempts to synthetically imitate this level of sequence control have thus far eluded chemists.[4-7] Advances have been seen in the form of the development of Single Unit Monomer Insertion,[8] which take advantage of differing bond stability to add precisely one monomer unit into a growing chain. This procedure is however synthetically laborious and at this stage only suitable for short oligomers. An alternative technique is the synthesis of multiblock copolymers by use of iterative reversible deactivation radical polymerization (RDRP) steps as pioneered in 2011.[9] This technique has been applied to a number of RDRP processes including atom transfer radical polymerisation (ATRP)[10-15], single electron transfer living radical polymerisation (SET-LRP)[16]. The key to success via this approach is the synthesis of each block to essentially full conversion while maintaining high livingness (end group fidelity). In recent years, this approach has been exploited quite extensively using reversible addition fragmentation chain transfer (RAFT) polymerization,[17-22] as exemplified by Gody *et al.*[17] who prepared an isodecablock (20 blocks) acrylamide copolymer.

In RAFT polymerization, initiation by a radical initiator produces new chains with additional chain ends. Bimolecular termination leads to the loss of an equal number of chains as that created from the initiator. The instantaneous number of chains that undergo bimolecular termination is dictated by the radical concentration and will be the same in all RDRP if the polymerization rate is the same. The degree of livingness thus directly correlates with the rate of generation of initiator radicals, given that all radicals lead to termination events. The degree of livingness in RAFT polymerization can therefore be increased by exploitation of polymerizations in dispersed systems such as miniemulsion and emulsion polymerizations. Such systems may be subject to compartmentalization effects, more specifically the segregation effect on propagating radicals, which reduces the termination rate and thereby increases the polymerization rate.[23-24] As a consequence, the rate of initiation (amount of initiator) can be reduced, thus leading to higher livingness. This has recently been demonstrated quantitatively by comparing RAFT polymerizations in miniemulsion and the corresponding homogeneous system.[25] Emulsion polymerization also exhibits another feature – exploited in the present work – which is the fact that the polymerization occurs in submicron-size polymer particles in the presence of micron-size monomer droplets. The monomer droplets act as monomer reservoirs and supply monomer to the polymer particles as the polymerization proceeds. As such, there is a self-regulatory effect such that the monomer concentration is kept relatively low in the polymer particles compared to the corresponding homogeneous system.[23] Engelis *et al.*[26] prepared methacrylate-based multiblock copolymer using "sulfur-free RAFT" emulsion polymerization employing methacrylate-type macromonomers using a semi-continuous process relying on maintaining a low monomer concentration by use of a continuous monomer feed. Methacrylate macromonomers have very low exchange coefficients compared to "normal" RAFT agents, and

it is thus crucial to minimize the monomer concentration to achieve living characteristics (low number of monomer units added per activation-deactivation cycle). This concept was established in earlier work by Moad and coworkers, who demonstrated that methacrylate-based copolymers (up to 6 blocks) can be synthesized using the methacrylate macromonomers as "sulfur-free RAFT" in emulsion polymerization.[27-30]

Ferguson *et al.* first demonstrated that RAFT polymerization can be elegantly implemented as an *ab initio* emulsion polymerization by use of amphiphilic macroRAFT agents formed *in situ.*[31] The amphiphilic macroRAFT agents self-assemble into aggregates (micelles) that swell with monomer, and subsequent polymerization within these entities lead to particle formation. This technique also allows for moieties in the starting diblock to be expressed on the outside of the nanoparticles formed, thus allowing for surface functionalisation.[32] Polymerization-induced self-assembly (PISA) relies on the same principle of self-assembly, *i.e.* the solvophobic block is generated *in situ*, but typically under conditions such that non-spherical morphologies can also be obtained.[33-34] We have recently reported that RAFT emulsion polymerization using an amhiphilic macroRAFT agent allows access to complex multiblock copolymer particles exhibiting multilayered morphology.[22] We have also recently demonstrated that high-order (decablock) methacrylate-based multiblock copolymers can be prepared efficiently at high polymerization rates using an amphiphilic macroRAFT agent also in case of slowly propagating monomers such as methacrylates by exploitation of the compartmentalization effect in emulsion polymerization.[35]

To date, the very vast majority of macroRAFT agents employed in emulsion polymerization based on the PISA concept have either a hydrophilic R-group (with this R-group becoming amphiphilic *in situ* as the hydrophobic monomer polymerizes) or an amphiphilic R-group comprising for example a polystyrene block and a poly(acrylic acid) block. MacroRAFT agents that simultaneously possess a solely hydrophobic Z- and hydrophilic R-group have received less attention. Stoffelbach et al.[36] employed the surface active low molecular weight trithiocarbonate RAFT agent 2-(dodecylthiocarbonothioylthio)-2-methylpropanoic acid in emulsion polymerization. In the case of homopolymerization of methyl methacrylate (MMA), uniform nanoparticles were produced but the molecular weight distributions (MWDs) were broad, although copolymerization with small amounts of styrene or *n*-butyl acrylate (nBA) resulted in good control. In subsequent work, Rieger et al.[37-38] explored the use of a macroRAFT agent where the carboxylic R-group was replaced with a hydrophilic poly(ethylene oxide) (PEO) segment, rendering the homopolymerizations of both styrene and nBA successful. However, poor control over the MWD was obtained in case of methacrylates, but copolymerization of nBA/MMA proceeded well. This was at the time not surprising given that this RAFT agent is incompatible with methacrylates – this issue will be revisited in the present work.

We have herein explored the use of a macroRAFT similar to that previously studied by Rieger et al.[37-38], *i.e.* a trithiocarbonate with a hydrophilic R-group in the form of a PEO segment and a hydrophobic dodecyl moiety as the Z-group. The focus has been on how the heterogeneus nature of emulsion polymerization can influence the progression of the polymerization in comparison to model miniemulsion- and solution

polymerizations. It is demonstrated that the in-built monomer feeding mechanism of emulsion polymerization provides a dramatic increase in RAFT control ($Đ \leq 1.15$) for methacrylate polymerization. This strategy was exploited for synthesis of sequence-controlled methacrylate multiblock copolymers by RAFT *ab initio* emulsion polymerization.

Experimental

Materials

The commercial RAFT agent (CTA-acid, Scheme 1) was provided by Lubrizol and recrystallized from warm hexane before use. Oxalyl chloride DCM solution, SDS and 2k MeO-PEG-OH were purchased from Sigma Aldrich and used as provided. Butyl acrylate (BA), butyl methacrylate (BMA), methyl methacrylate (MMA) and hexyl methacrylate (HMA), were purchased from Sigma Aldrich and passed through a short aluminium oxide column to remove inhibitor prior to use. The initiators 2,2'-azobis[N-(2-carboxyethyl)-2-methylpropionamidine]tetrahydrate (VA-057), 4,4'-azobis(4-cyanopentanoic acid) (ACPA), azobisisobutyronitrile (AIBN) were purchased from Wako chemicals and used as provided. The solvents dichloromethane (DCM), dimethylformamide (DMF) and dioxane were purchased from Fisher.

NMR

^{1}H NMR spectra were recorded on a Bruker Avance 300 spectrometer (300 MHz) at 21 °C in $CDCl_3$. For ^{1}H NMR spectroscopy, the delay time (d1) was 2 s. Chemical shift values (δ) are reported in ppm downfield of a TMS standard. Mestrenova software was used to analyze the results.

SEC

SEC was performed on an Agilent Infinity II MDS instrument equipped with differential refractive index (DRI) and multiple wavelength UV detectors, one of which is set to 309 nm. The column used for separation is a PLgel Mixed C columns (300 x 7.5 mm) and a PLgel 5 µm guard column. The eluent is THF containing 2 % v/v triethylamine (TEA) and 0.01 % v/v butylated hydroxytoluene (BHT) at 1 ml min^{-1} and 30 °C. Analyte samples were filtered through a GVHP membrane with 0.22 µm pore size before injection. Experimental molar mass ($M_{n,exp}$) and dispersity ($Đ$) values of synthesized polymers were determined based on PMMA conventional calibration using Agilent GPC/SEC software.

Dynamic Light Scatering (DLS)

DLS measurements were performed on a MALVERN Zetasizer Nano ZS operating at 25 °C with a 4 mW He-Ne 633 nm laser module. Measurements were made in back scattering mode at an angle of 173°. Measurements were performed in triplicate with automatic attenuation selection and measurement position. The results were analysed using Malvern DTS 6.20 software.

PEG-CTA Synthesis

1.37 g CTA-acid (3 eq, 3.76 mmol) was dissolved in 2.813 mL of oxalyl chloride DCM solution (2M) (4.5 eq, 5.64 mmol) to yield a bright yellow solution. 3 drops of anhydrous DMF was added to this solution resulting in rapid gas generation and a change in colour to orange. After effervescence had stopped, the solution was sealed and gently stirred at room temperature for 1 h. Separately 2.5 g 2k MeO-PEG-OH (1 eq, 1.25 mmol) was dissolved in 10 mL of DCM, this was then added to reaction and left stirring overnight to yield a dark yellow solution. The product was then obtained by precipitating this solution into an 80:20 mix of hexane and diethyl ether followed by drying overnight at 40 °C under vacuum to afford a pale yellow powder (H^1 NMR in Fig. SI1) (Yield = 2.63 g 89%). ^{1}H NMR ($CHCl_3$, 300 MHz) δ 4.27 2H $COOC\mathbf{H}_2CH_2O$ t 6 Hz, 3.89 2H $COOCH_2C\mathbf{H}_2O$ t 6 Hz, 3.66 176H $(OC\mathbf{H}_2C\mathbf{H}_2)_{44}$ m, 3.40 3H $OCH_2CH_2OC\mathbf{H}_3$ s, 3.28 2H $SCSSC\mathbf{H}_2CH_2$ t 5 Hz, 1.71 6H $S(C\mathbf{H}_3)_2CCOOCH_2$ s J, 1.65 2H $SCSSCH_2C\mathbf{H}_2$ tt 5,2 Hz, 1.27 18H $SCSSCH_2CH_2(C\mathbf{H}_2)_9CH_3$ m, 0.90 3H $CH_2CH_2C\mathbf{H}_3$ t 9 Hz. MS [M + Na^+] calculated as 2369.2 found as 2368.9.

CTA-1 Synthesis

2.5 g CTA-acid (1 eq, 6.86 mmol) was dissolved in 5.12 mL of oxalyl chloride DCM solution (2M) (1.5 eq, 5.64 mmol) to yield a bright yellow solution. 3 drops of anhydrous DMF was added to this solution resulting in rapid gas generation and a change in colour to orange. After effervescence had stopped, the solution was sealed and gently stirred at room temperature for 1 h. After this time, a large excess of butan-1-ol (c.a. 50 mL) was added to the solution and left stirring unsealed overnight. Stirring was then stopped and the product, a red-orange oil, was observed to phase separate from the solution and was collected with use of a separating funnel (Yield = 2.10 g 73%). ^{1}H NMR ($CHCl_3$, 300 MHz) δ 4.13 2H $COOC\mathbf{H}_2CH_2CH_2$ t 6 Hz, 3.28 2H $SCSSC\mathbf{H}_2CH_2$ t 5 Hz, 1.71 6H $SC(C\mathbf{H}_3)_2COOCH_2$ s, 1.68 2H $COOCH_2C\mathbf{H}_2CH_2$ tt 6 Hz, 1.65 2H $SCSSCH_2C\mathbf{H}_2$ tt 5,2 Hz, 1.41 2H $COOCH_2CH_2C\mathbf{H}_2$ m, 1.27 18H $SCSSCH_2CH_2(C\mathbf{H}_2)_9CH_3$ m, 0.90 – 0.88 6H $SCSS(CH_2)_{11}C\mathbf{H}_3$ overlapped with $COOCH_2CH_2CH_2C\mathbf{H}_3$.

CMC Determination

30 µL of a 0.1 mg/mL solution of nile red in THF was transferred to ten 2 mL glass vials and dried in an oven at 40 °C for 48 hrs. Separately PEG-ester CTA solutions in water were prepared at the following concentrations; 50, 25, 10, 1, 0.1, 1 10^{-2}, 1 10^{-3}, 1 10^{-4}, 1 10^{-5}, 1 10^{-6} mg mL^{-1}. 2 mL of each PEG-ester CTA solution was then added separately to the Nile red containing vials. The vials were then sealed and placed on a roller at room temperature for a further 48 hrs. The fluorescence intensity of Nile Red was then measured on a BioTek cytation3 plate reader using an excitation wavelength of 560 nm and an emission wavelength of 600 nm.

Emulsion Polymerization

In a typical emulsion polymerization; 102.2 mg PEG-CTA (1 eq, 0.046 mmol) was dissolved in 5 mL of deionised water in a 20 mL glass vial, 0.727 mL BMA (0.649 g, 100 eq, 0.457 mmol) and 0.253 mL of a VA-

057 stock solution (0.01 g mL^{-1} H_2O) (2.53 mg 0.125 eq, 0.00610 mmol) were then added to the reaction. The vial was then sealed and briefly vortexed before purging with nitrogen gas for 15 min. The reaction was then heated to 70 ºC in a monitored oil bath and stirred at 500 RPM for 90 minutes to form a white latex. Samples for kinetic measurements were withdrawn periodically with a nitrogen purged syringe. For all other polymerizations targeting a degree of polymerization (DP) of 100, the amount of PEG-ester CTA, water and VA-057 stock solution was kept constant and the amount of monomer varied to give the same molar ratios. When targeting polymers of various DP, the ratio of PEG-ester CTA to VA-057 was kept constant and the amount of monomer varied with respect to the CTA.

Solution Polymerization

The rate of generation of radicals was adjusted to be approximately the same rate (relative to molar amount of RAFT agent) as in miniemulsion and emulsion by tuning the initial AIBN concentration (1.9 mmol L^{-1}) at monomer concentration of 0.8 M (entry SP1, Table 1). For the other experiments (SP2-4) the AIBN concentration was adjusted to keep the same RAFT/initiator ratio in all systems, while also keeping the same [BMA]/[RAFT]. In a typical experiment (SP1, Table 1) 18.6 mg of CTA-1 (1 eq, 0.044 mmol), 0.66 g BMA (103 eq, 4.6 mmol), 1.9 mg of AIBN (0.26 eq, 0.012 mmol), 36.3 mg of trioxane (9 eq, 0.40 mmol) and 5.1 ml of dioxane were mixed together in a 20 mL vial. The vial was sealed and degassed by purging nitrogen for 30 min followed by heating at 70°C for 22h. Samples were periodically withdrawn to monitor conversion by ^{1}H NMR (using trioxane as internal reference), M_n and $Đ$ as a function of time.

Miniemulsion Polymerization

In a typical miniemulsion experiment, organic phase was prepared by mixing 38.4 mg of CTA-1 (1 eq, 0.09 mmol), 1.45 mL BMA (1.3 g, 100 eq, 9 mmol) and 0.08 ml HD (0.065 g). The aqueous phase was prepared by dissolving 0.065 g of SDS into 9.5 ml of deionised water in a 25ml-vial. Organic phase was added to the aqueous phase and subsequently ultrasonicated using a Branson 450 probe (maximum output power of 500 W) at an amplitude of 50% for 10 min. Then 0.474 ml of a VA-057 stock solution (0.01 g/mL H_2O) (4.74 mg, 0.125 eq, 0.011 mmol) was added to the reaction mixture. The vial was sealed and purged with nitrogen gas for 30 minutes. The reaction mixture was then heated to 70ºC for 90 min. Samples were periodically withdrawn to monitor conversion (gravimetric analysis), particle size, M_n and $Đ$ as function of time.

Results and Discussion

RAFT emulsion polymerization. The macroRAFT agent with a hydrophilic R- and hydrophobic Z-group was synthesised by first converting the commercial CTA-acid to the acid chloride equivalent *in situ*, followed by immediate further reaction with PEG-OH (Scheme 1).

Scheme 1. Synthesis of PEG-ester CTA from CTA-acid.

DLS was used to investigate the self-assembly of the PEG-ester CTA in water. A single unimodal peak was observed with an intensity-average diameter of 21 nm, consistent with the formation of micelles (Fig. SI2). The critical micelle concentration (CMC) was measured using a Nile red assay,[39] which relies on the increase in fluorescence of Nile red dye when in a hydrophobic environment. This assay (Fig. SI3) gave a CMC value of 0.161 mg mL^{-1} (6.98 10^{-5} mol L^{-1}) at 298 K, markedly lower than small molecule commercial surfactants such as SDS and Brij-35[40-41] and in line with polymeric surfactants CMC values (in the range 10^{-9} – 10^{-4} mol L^{-1}) and literature values.[37, 42-43]

The PEG-ester CTA was then used as the surfactant for a BA emulsion polymerization based on the experimental conditions in Table 1 (entry EP1); in all cases the concentration of PEG-ester CTA was fixed at 8.04 mmol L^{-1}, *i.e.* above its CMC value.[44] The polymerization proceeded rapidly with 99% conversion reached in 1.5 h. A stable latex was obtained with DLS (Fig. SI4) showing nanoparticles with a Z-average diameter of 120 nm and a particle dispersity index (*PDI)* of 0.015. Gel permeation chromatography revealed a low dispersity peak (Figure 1A, $Đ$ = 1.14) with $M_{n,exp}$ (16,000 PMMA equivalents) ≈ $M_{n,th}$, suggesting good control and showing that PEG-ester CTA can function as both an effective surfactant and a RAFT agent (EP1, Table 1) in agreement with previous work by Charleux and coworkers for PEG-ester CTA/nBA.[37]

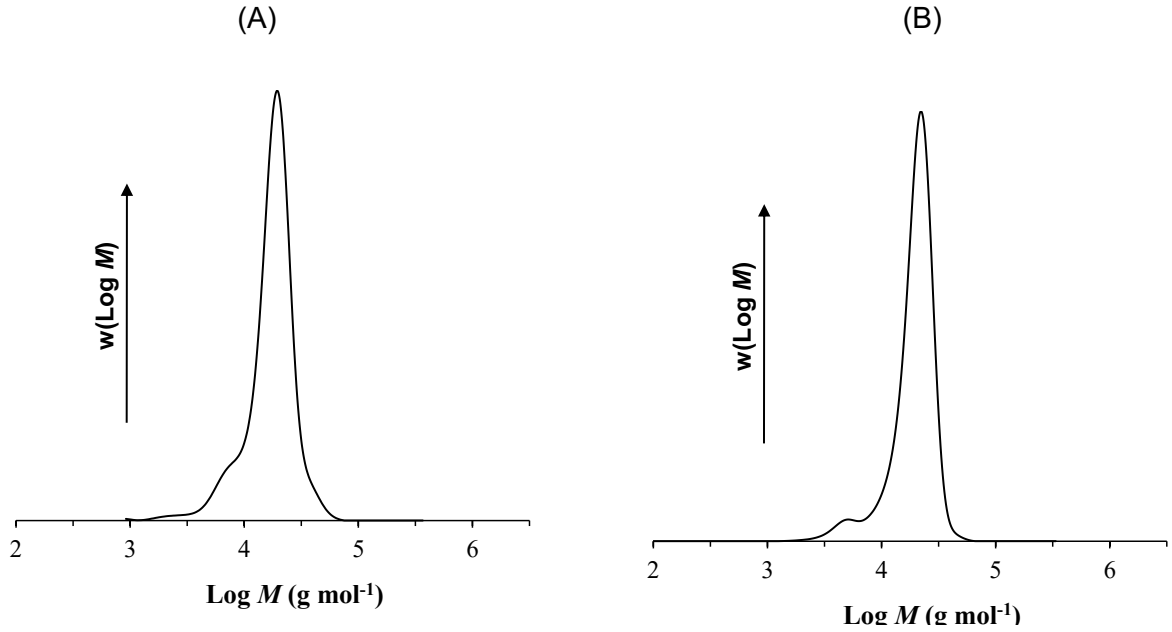

Figure 1: Molecular weight distributions for PBA_{100} (A) and $PBMA_{100}$ (B) (EP1 and EP2 in Table 1, respectively).

Following the successful application of PEG-ester CTA to the polymerization of butyl acrylate, butyl methacrylate (BMA) was next investigated (EP2, Table 1). Unlike with butyl acrylate, the PEG-ester CTA was not expected to control the polymerization of a methacrylate due to a R-group that is not appropriate for methacrylate polymerization.[45] This polymerization also proceeded at a high rate with 99% conversion in 1.5 h, generating a stable latex with Z_{av} = 75 nm and PDI = 0.05 ((EP2, Table 1). Surprisingly, the MWD was monomodal ($Đ$ = 1.14; Fig. 1B), although displaying a slight low molecular weight shoulder, also present in the polymerisation of butyl acrylate (EP1). The low molecular weight shoulder aligns with the molecular weight of the initial PEG-ester CTA, suggesting it corresponds to either unreacted RAFT agent or dead chains. SEC using a UV detector set at 309 nm confirmed the presence of trithiocarbonate end groups in this low molecular weight shoulder, strongly suggesting it relates to unreacted RAFT agent. The experimental M_n values exhibited good agreement with the theoretical values ($M_{n,th}$ = 16,520 and $M_{n,exp}$ = 16,000, Table 1), confirming successful RAFT polymerization.

This surprising result was confirmed by polymerizing other methacrylate monomers under the same conditions (entries EP3-4, Table 1, Fig. SI4). There was generally a good agreement between $M_{n,th}$ and M_n determined by SEC (Table 1) with low $Đ$ values. A notable exception to this is hexyl methacrylate (EP4, Table 1), in which case $M_{n,exp} < M_{n,th}$, although this is most likely due to the use of inappropriate PMMA standards for GPC calibration. Successful RAFT polymerization of various methacrylate monomers (BMA, MMA and HMA, entries EP2-4 in Table 1, respectively) was thus achieved. The good control over MMA polymerization came as a surprise, since Charleux and coworkers[37-38] had shown that a similar system did not control MMA polymerization. Upon close inspection of the system, it appears that the choice of initiator is key to controlling the polymerization. Indeed, Charleux and co-workers used an anionic radical initiator, ACPA (in solution above its pKa, neutralized by 3.5 molar equiv of $NaHCO_3$), whilst we used a non-ionic initiator, VA-057 (natural pH, non-neutralized). In order to investigate this effect, we undertook polymerizations of MMA and BMA using PEG-ester CTA and ACPA as initiator (0.125 molar equiv of ACPA). We confirmed reasonable control over BMA polymerization, whilst MMA polymerization is poorly controlled, as illustrated by size exclusion chromatography showing a bimodal pMMA MWD, with a narrow peak corresponding to unconsumed PEG-ester CTA, and a second broad peak from the uncontrolled PMMA (Fig. SI6).

The lack of control over the polymerization and lack of complete RAFT agent consumption are attributed to secondary nucleation events. In this system, the fairly water-soluble MMA oligomers formed at the start of the reaction continue to grow in the aqueous phase rather than entering a preformed micelle. Beyond a critical chain length, these oligomers provide an alternative locus for the emulsion polymerization to take place. Importantly these separate polymerization loci do not contain any PEG-ester CTA, thus explaining both the poor control and lack of RAFT agent consumption. In the case of the more hydrophobic BMA, less secondary nucleation takes place leading to improved polymerization control and greater RAFT agent consumption. In

the case of the polymerizations initiated by VA-057, secondary nucleation events are minimised even for MMA polymerizations, as the lack of charge on the oligomers enhance their insolubility, thus promoting rapid micellar entry and preventing secondary nucleation.

Nevertheless, control over methacrylate derivatives was surprising, given the reinitiating group (R-group) is well established to be inappropriate for methacrylate monomers in homogeneous (bulk/solution) systems,[45] and warranted further investigation. The R-group of PEG-ester CTA is very similar in structure to that of the PMMA propagating radical (which is the R-group in MMA RAFT polymerization after the main equilibrium has been established) – the main difference near the radical centre being a methyl substituent (PEG-ester CTA) having been replaced with the PMMA chain – however this apparently has a significant impact on the RAFT kinetics.

RAFT solution and miniemulsion polymerizations

The R group effect was therefore further investigated by performing polymerizations using the same conditions as in the emulsion polymerizations but under miniemulsion polymerization conditions (ME1, Table 1). In a miniemulsion polymerization, polymer particles are generated directly from pre-formed submicron-sized monomer droplets.[46] This is fundamentally different from an emulsion polymerization, where particle formation occurs in the aqueous phase followed by monomer transport from micron-sized monomer droplets via diffusion through the aqueous phase to the polymer particles, where polymerization occurs. A similar RAFT agent (same Z-group and same radical nature of the R-group) was employed, but the PEG group attached to the R-group was replaced by the hydrophobic moiety -C_4H_9 (CTA-1; Scheme 2). This modification in the CTA structure was necessary in order to obtain a hydrophobic RAFT agent which will be located in the monomer droplets after the ultrasonication step (*i.e.* not at the droplet/water interphase nor in the aqueous phase as the case would be for the PEG-based RAFT agent).[47] In addition, a third set of experiments was carried out in the form of solution polymerizations in dioxane using the CTA-1 (SP1-4, Table 1) with AIBN as initiator (VA057 was employed for the emulsion and miniemulsion polymerizations, but this initiator is not soluble in dioxane). The initial concentrations of AIBN and VA057 were adjusted (Table 1) in all polymerizations in order to obtain approximately the same rate of radical generation (Fig. SI 7) relative to the molar amount of RAFT agent at 80ºC during the initial 1.5h of polymerization (the time required to obtain near full conversion in the emulsion and miniemulsion systems). The target DP of BMA (100) was kept the same for the three systems (constant [BMA]:[RAFT].

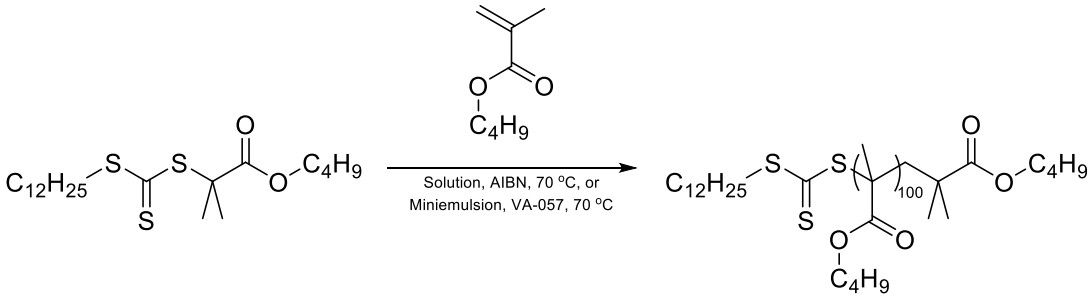

Scheme 2. RAFT polymerization of BMA in solution and miniemulsion using CTA-1 as RAFT agent (experimental conditions in Table 1).

Table 1. Experimental conditions and results for RAFT polymerizations of various monomers in emulsion (using PEG-ester CTA; Scheme 1), miniemulsion and solution (using CTA-1; Scheme 2).

Exp.	Mon	$[Mon]_0$ (mol L^{-1})[a]	[RAFT]/[I]	X (%)/ t (h)	$M_{n,th}$ (g mol^{-1})	$M_{n,exp}$ (g mol^{-1})	$Đ$	Z_{av} (nm) / PDI
Miniemulsion polymerization								
ME1	BMA	6.5	8	99/1.3	14,400	23,400	2.30	120/0.03
Emulsion polymerization								
EP1	BA	0.8	8	99/1.5	15,177	16,500	1.14	120/0.02
EP2	BMA	0.8	8	99/1.5	16,520	16,000	1.13	75/0.05
EP3	MMA	0.8	8	99/1.5	12,312	9,000	1.10	60/0.39
EP4	HMA	0.8	8	99/1.5	19,325	32,000	1.09	85/0.05
Solution polymerization								
SP1	BMA	0.8	4	83/22	12600	16700	1.80	-
SP2	BMA	2.0	4	96/22	14900	19200	1.84	-
SP3	BMA	3.2	4	99/22	15800	21200	1.78	-
SP4	BMA	4.1	4	100/22	14600	17300	1.74	-

Table 1 – T = 70°C; [BMA]/[CTA-1] = 100; VA057 used as initiator for emulsion/miniemulsion polymerizations, AIBN was used for solution (1,4-dioxane) polymerization; Concentrations of AIBN/VA057 adjusted to give same (approx.) rates of radical generation for the first 90 min (profiles of initiator decomposition in Fig. SI7). Solid content of miniemulsion = 20 wt%; SDS = 5 wt% relative to monomer; HD = 5 wt% relative to monomer; Conversion determined gravimetrically for miniemulsion and by ^{1}H NMR for solution and emulsion polymerization. [a] Organic (dispersed) phase monomer concentration.

As expected, the segregation effect[48] (observed in miniemulsion and emulsion systems with sufficiently small particles) plays a crucial role in the kinetics of the polymerization - in these systems full conversion was obtained after only 1.5 h, while the polymerization rate was much lower for the solution polymerizations (SP1 and SP4, Fig. 2; zoomed in version in Fig. SI8). The segregation effect leads to a lower rate of termination, and consequently a higher polymerization rate. The solution polymerization with an initial monomer concentration of 4.1 M is comparable to the corresponding miniemulsion polymerization in the sense that the overall monomer concentration in solution is similar to the monomer concentration in the initial monomer droplets in the miniemulsion (approx. 6 M) (the [BMA]/[CTA-1]/[AIBN] ratio was kept constant

in SP1-4). In ideal miniemulsion polymerization, each monomer droplet is converted to a polymer particle ("one-to-one copy"). The approximately constant droplet/particle size during the polymerization (Fig. SI 9) at Z_{av} = 120 nm (similar to the final particle size of the emulsion polymerizations) is consistent with predominant droplet nucleation as expected. The evolution of M_n with conversion was also monitored (Figure 3), solution polymerisations (SP1, SP4) and miniemulsion (ME1) show a rapid increase in M_n at low conversion followed by a plateau; characteristic of uncontrolled free radical polymerisation. The M_n value meanwhile, for the emulsion polymerisation (EP2), shows the linear increase with conversion expected for a controlled radical process. Interestingly at low conversion (<20%), M_n increases faster than expected for EP2, this correlates well with the prenucleation stage of an emulsion polymerisation where it is still effectively free radical.

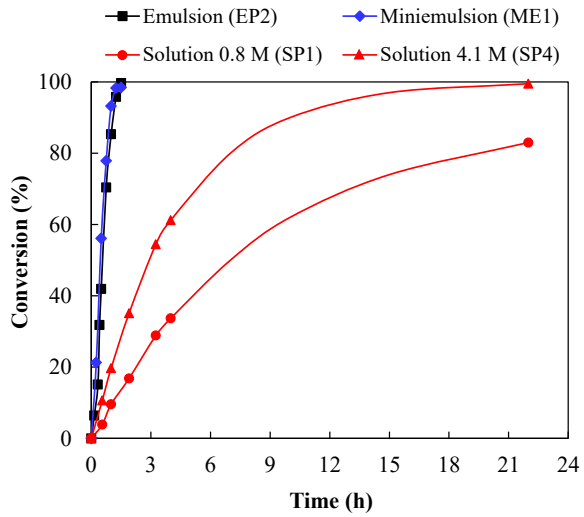

Figure 2 – Conversion-time data for RAFT polymerization of BMA at 70 °C via emulsion, miniemulsion and solution polymerization (EP2, ME1, SP1 and SP4 in Table 1).

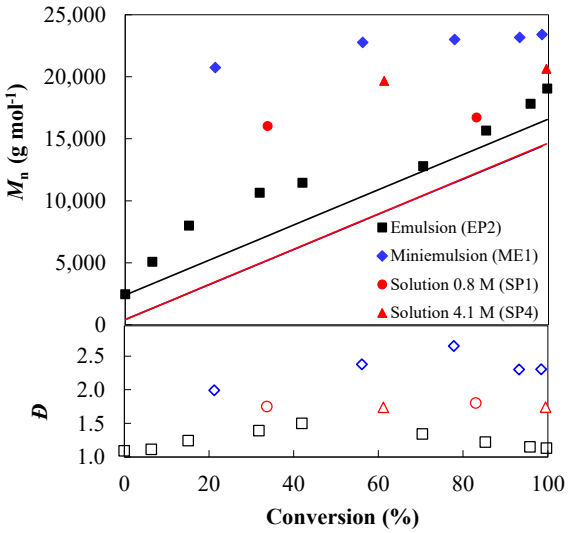

Figure 3 – Evolution of M_n and $Đ$ with conversion for RAFT polymerization of BMA at 70 °C via emulsion, miniemulsion and solution polymerization (EP2, ME1, SP1 and SP4 in Table 1). Black line is $M_{n,th}$ for emulsion polymerization, whereas red

line is $M_{n,th}$ for solution and miniemulsion polymerizations (these differ due to the initial M_n of the RAFT agents being different).

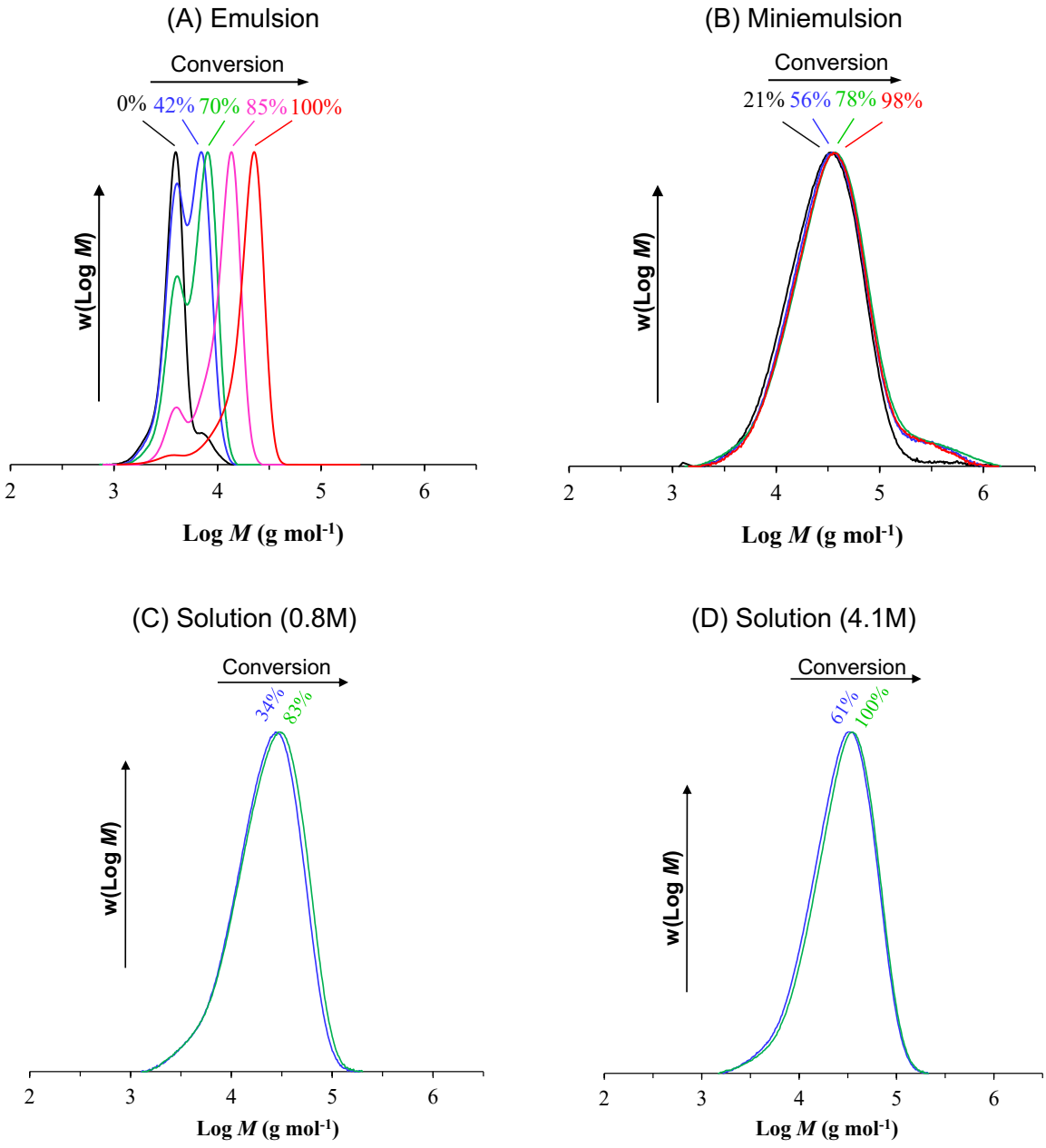

Figure 4 – Molecular weight distributions of RAFT polymerization of BMA at 70ºC via (A) emulsion, (B) miniemulsion and (C,D) solution polymerizations at [BMA] = 0.8 and 4.1M (entries EP1, ME1, SP1 and SP4, respectively, Table 1).

The miniemulsion and solution polymerizations were clearly not under RAFT control. The MWs remained approximately constant with conversion and the dispersities were high (Figure 3 and 4; $Đ > 1.7$). This behaviour has previously been reported for homogeneous systems (solution/bulk),[36, 49] and can be attributed to the chain transfer constant (C_{tr}) being too low ($C_{tr} \approx 11$) for methacrylates and RAFT agents with similar R group generating tertiary radicals (·**C**$(CH_3)_2$-COO-CH_2-CH_3).[36, 49] Surprisingly, however, the emulsion polymerization system exhibited the characteristic features of control/livingness.

Mechanistic considerations

How is it that the polymerization proceeds without control in solution/miniemulsion, whereas very good control is achieved in the corresponding emulsion polymerization? The problem with C_{tr} being too low can in fact be overcome in an emulsion polymerization under appropriate conditions[50]. In an emulsion polymerization, the ratio of monomer concentration to RAFT agent concentration at the polymerization locus (*i.e.* in the polymer particles) is lower than the overall [M]/[RAFT] across the entire system due to the presence of monomer droplets (inside which no polymerization occurs). In order to quantitatively illustrate this point, we have calculated the ratio of [M]/[RAFT] at the polymerization locus for the three different systems as a function of overall monomer conversion. In the case of solution polymerization, the polymerization locus refers to the entire solution phase, whereas in the case of miniemulsion polymerization the monomer droplets / polymer particles constitute the polymerization locus (in a miniemulsion polymerization, monomer droplets are directly converted to polymer particles).[46] The monomer concentration as a function of conversion for miniemulsion and solution polymerization is given by:

$$[\mathrm{M}]_{Locus} = (1 - X) \times [\mathrm{M}]_0 \quad (1)$$

where X is the fractional conversion and $[\mathrm{M}]_0$ the initial monomer concentration. However, in case of an emulsion polymerization, the monomer concentration must be calculated using different approaches depending on the Interval of the emulsion polymerization (Eq. 2-4). Interval I is the nucleation stage (generation of particles). Interval II refers to the particle growth stage, where monomer diffuses from micron-sized droplet to the particles, maintaining the thermodynamic equilibrium, which results in a close to constant monomer concentration inside the monomer-swollen particles despite monomer being consumed by propagation. Interval III begins when the monomer droplets have been depleted; the monomer concentration in the particles decreases as the polymerization proceeds during this stage.[51-52]

$$\text{Interval I: } [\mathrm{M}]_{Locus} = [\mathrm{M}]_w \quad (2)$$

$$\text{Interval II: } [\mathrm{M}]_{Locus} = [\mathrm{M}]_{sat} \quad (3)$$

$$\text{Interval III: } [\mathrm{M}]_{Locus} = (1 - X) \times [\mathrm{M}]_0 \quad (4)$$

where $[M]_w$ is the saturated monomer concentration in water (for BMA, 7.0 mmol L^{-1}).[53] Interval I was assumed to be completed at 10% conversion.[51-52] The beginning of Interval III was taken as the point when the monomer concentration based on Eq. 4 becomes lower than the saturated monomer concentration in the particles ($[M]_{sat}$; see below). The extent of swelling of polymer particles with monomer under conditions of thermodynamic equilibrium (excess monomer present, *i.e.* monomer droplets present) is denoted $[M]_{sat}$. Although $[M]_{sat}$ is generally considered constant during Interval II, the extent of swelling of polymer particles with monomer does depend on particle size for sufficiently small particles – this effect is particularly strong for diameters less than 60 nm (Fig. SI 10).[54-55] The pressure arising from the surface tension causes a decrease in the monomer concentration and this effect is more significant for small particles[54] as initially proposed by Morton *et al*.[56] The Morton Equation (Eq 5) provides a theoretical basis for prediction of $[M]_{sat}$:

$$\ln(1-\varphi_p)+\varphi_p+\chi\,\varphi_p{}^2+\frac{2\,\Gamma\,V_{sM}}{r_u RT}\varphi_p{}^{1/3}=0 \qquad (5)$$

where Γ is the interfacial tension between the latex particle and the aqueous phase, φ_p is the volume fraction of polymer in the latex particle, V_{sM} is the partial molar volume of monomer, χ is the Flory-Huggins interaction parameter and r_u is the radius of the unswollen particle. However, estimation of $[M]_{sat}$ as a function of particle size based on the Morton equation can be a laborious task. In the present work, $[M]_{sat}$ was estimated as a function of the average particle diameter by using a semi-empirical iterative approach based on the Morton Equation (fully described in the Supplementary Information). Figure 5A shows the thus obtained values of $[M]_{Locus}$ (here denoted $[BMA]_{Locus}$) as a function of conversion for the three systems: emulsion, miniemulsion and solution polymerization.

Understanding of the kinetics also requires knowledge of the concentration of RAFT moieties at the locus of polymerization. The RAFT concentration at the polymerization locus ($[RAFT]_{Locus}$) was calculated as follows:

$$[\mathrm{RAFT}]_{Locus}=n_{\mathrm{RAFT}}/V_{Locus} \qquad (6)$$

where n_{RAFT} is the initial number of moles of macroRAFT and V_{Locus} is the total volume of the system for the solution polymerization, the total volume of the monomer swollen particles for emulsion polymerization (more details in SI) and the total volume of droplets/particles for the miniemulsion system. The resulting plots of $[RAFT]_{Locus}$ as a function of conversion for the three systems are shown in Figure 5B.

It can be observed in Figure 5C that the [BMA]/[RAFT] ratios for emulsion polymerization are significantly lower than for the solution and miniemulsion systems. This difference can be ascribed to two effects: [BMA] and [RAFT] at the polymerization locus. As seen in Figure 5A, the $[BMA]_{Locus}$ for the emulsion polymerization system is lower than in miniemulsion contributing to the decrease of [BMA]/[RAFT] ratio, caused by the presence of micron-sized monomer droplets in the emulsion polymerization (Interval I and II). These monomer droplets merely serve as monomer reservoirs, and supply monomer to the polymer particles via diffusion through the aqueous phase as per the well-established mechanism of an emulsion

polymerization.[23, 52] As such, the monomer in the monomer droplets cannot react with propagating radicals (there is no droplet nucleation in conventional emulsion polymerization system), and a significant fraction of monomer is thus "excluded" from the system during Interval I and II. However, in addition to this, the $[RAFT]_{Locus}$ is much higher in Interval II of the emulsion polymerization system than in the miniemulsion (Figure 5B), which also contributes to the decrease in the [BMA]/[RAFT] ratio. This difference in $[RAFT]_{Locus}$ can be explained by the gradually growth of the particles in emulsion polymerization, and consequently low particle volume in intervals I and II, which results in a higher $[RAFT]_{Locus}$. In an ideal miniemulsion system ("1:1 copy"), the volume of the droplet/particle remains constant during the polymerization, resulting in a constant $[RAFT]_{Locus}$. Interestingly, and perhaps counterintuitive, the $[RAFT]_{Locus}$ (as opposed to [M]) is in fact the dominant factor in causing the reduction in $[BMA]_{Locus}/[RAFT]_{Locus}$.

The lower [BMA]/[RAFT] ratio in the emulsion polymerization system (Figure 5C) leads to the addition of fewer monomer units per activation/deactivation cycle, which in turn results in lower dispersities[57] and experimental M_n closer to the theoretical ones (Figure 3). If C_{tr} is sufficiently low, unreacted initial RAFT agent leads to $M_n < M_{n,th}$ (see Figure 3). This is an important result which shows that by exploiting emulsion polymerization, it is not only possible to enhance the polymerization rate via the segregation effect, but also improve control for a RAFT system that is not optimal for a given monomer. It is also important to highlight that the segregation effect (less termination due to physical isolation of propagating radicals) is operative both in the present miniemulsion and emulsion polymerization systems, but this is not the reason the RAFT system operates satisfactorily in the emulsion system. The segregation effect merely leads to an increase in polymerization rate, but cannot remedy the issue of the value of C_{tr} being too low as evidenced by the miniemulsion polymerization not performing well.

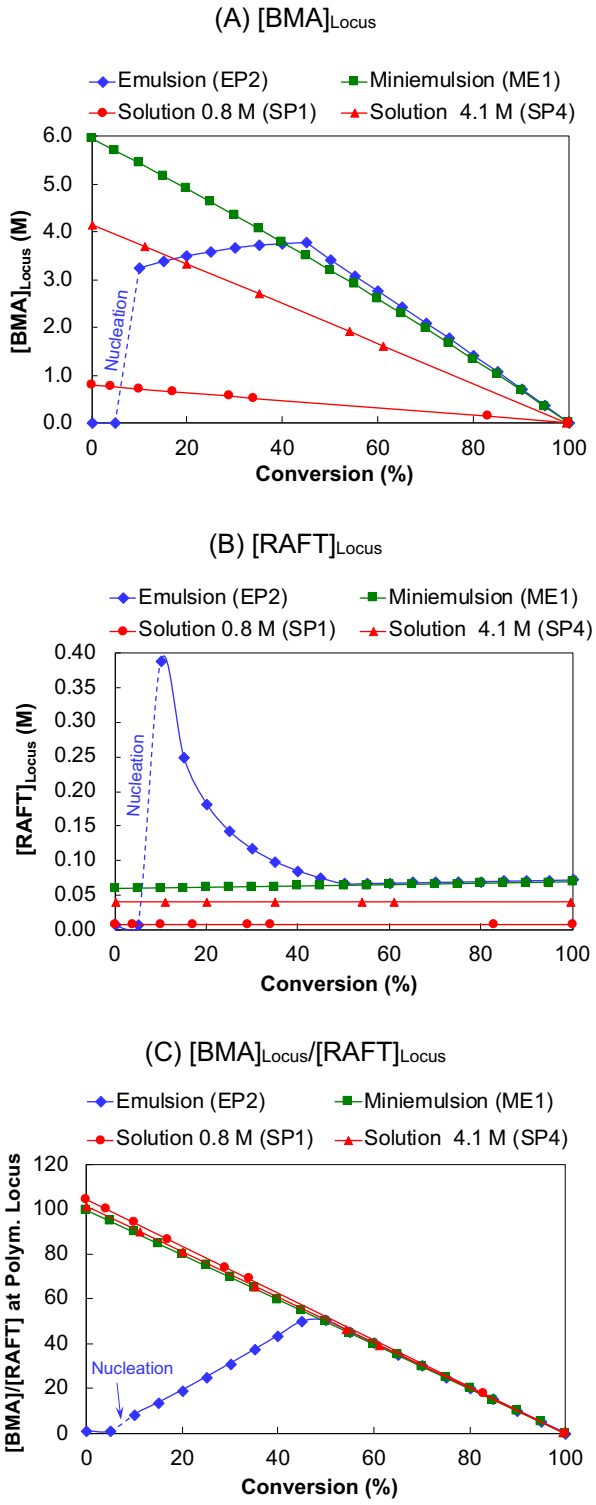

Figure 5 – Calculated values of (A) [BMA], (B) [RAFT] and (C) [BMA]/[RAFT] in the polymerization locus: particles and droplets/particles for heterogeneous systems and solvent for homogeneous system (Equations 1-6).

This feature, a lower [M]/[RAFT] ratio in emulsion polymerization, has previously been exploited by Moad *et al.*[29] to synthesize PS-*b*-PMMA block copolymer in the "wrong" polymerization sequence (the "correct" order should be MMA polymerized first then styrene forming PMMA-*b*-PS). The authors demonstrated that by controlling the feed rate of monomer in semi-continuous emulsion polymerization process, the concentration of monomer was kept sufficiently low, thus allowing the synthesis of the block copolymer in

the "wrong" order. The problem when the order is "wrong" is that the initial adduct radical (in the pre-equilibrium step) preferentially fragments to regenerate the PMMA radical. However, when the MMA concentration is kept low, fewer MMA units are added during each activation cycle, and consequently this problem becomes less significant, given that the adduct radical eventually fragments the "right" way. Recently, this concept was also successfully employed to the synthesis of methacrylate-based multiblock copolymers.[26, 58] Based on the strategy previously reported by Moad and co-authors,[27-30] methacrylate-based macromonomers were used as "sulfur-free" RAFT agents in emulsion polymerization using a continuous monomer feed process via syringe pump to keep the monomer concentration low.

It is noteworthy, that the control achieved in the emulsion polymerizations in the present work is of very high quality with $Đ$ values < 1.14 and as low as 1.09 for EP4 (Table 1). One additional aspect that may play a role in achieving this high level of control over the MWD is that the R-group of the initial RAFT agent PEG-ester CTA is hydrophilic - the thioester moiety is positioned between the hydrophilic and hydrophobic sections of the macroRAFT. As a consequence, once a z-mer[55] (radical entering from the aqueous phase) adds to this RAFT agent, the expelled R-radical is likely to exit the micelle/particle into the aqueous phase. Subsequent propagation in the aqueous phase would eventually lead to entry into another micelle/particle. Such "radical mobility" between has been reported to lead to more efficient nucleation of micelles,[59] which in turn leads to a situation where "all" particles nucleate at a similar rate allowing for synchronised chain growth as opposed to some chains being "left behind" in non-nucleated micelles. A similar phenomenon has previously been reported for a system related to a microemulsion polymerization,[59] and this feature of a surface active RAFT agent influencing the entry process has been termed "frustrated entry".[60-61]

Effect of particle size on [BMA]/[RAFT] ratio in RAFT emulsion

As discussed above, the extent of monomer swelling of the particles is directly affected by the particle size, especially for small particles (diameter ~40-100 nm). Therefore, we decide to investigate how this effect can quantitatively influence [BMA]/[RAFT] within particles. $[BMA]_{Locus}$ was calculated using equations 2-4 and equation SI3 (further details on SI) simulating systems with different diameters (50, 75, 100 and 150 nm) - the results are plotted in Figure 6A. The RAFT concentration and [BMA]/[RAFT] ratio at the locus of polymerization were also calculated (Figure 6B and C). As expected, the smaller the particle size, the lower the monomer concentration in the particles is (Figure 6A). However, the particle size does not strongly influence $[RAFT]_{Locus}$ (Figure 6B), only leading to a slight decrease in [BMA]/[RAFT] ratio with decreasing particle size (Figure 6C). It is also interesting to note that the point (conversion) at which the emulsion polymerization becomes equivalent to a solution/miniemulsion polymerization (beginning of Interval III) shifts to higher conversion with decreasing particle size due to smaller particles being unable to swell to the extent of larger particles (monomer droplets remain to higher conversion.

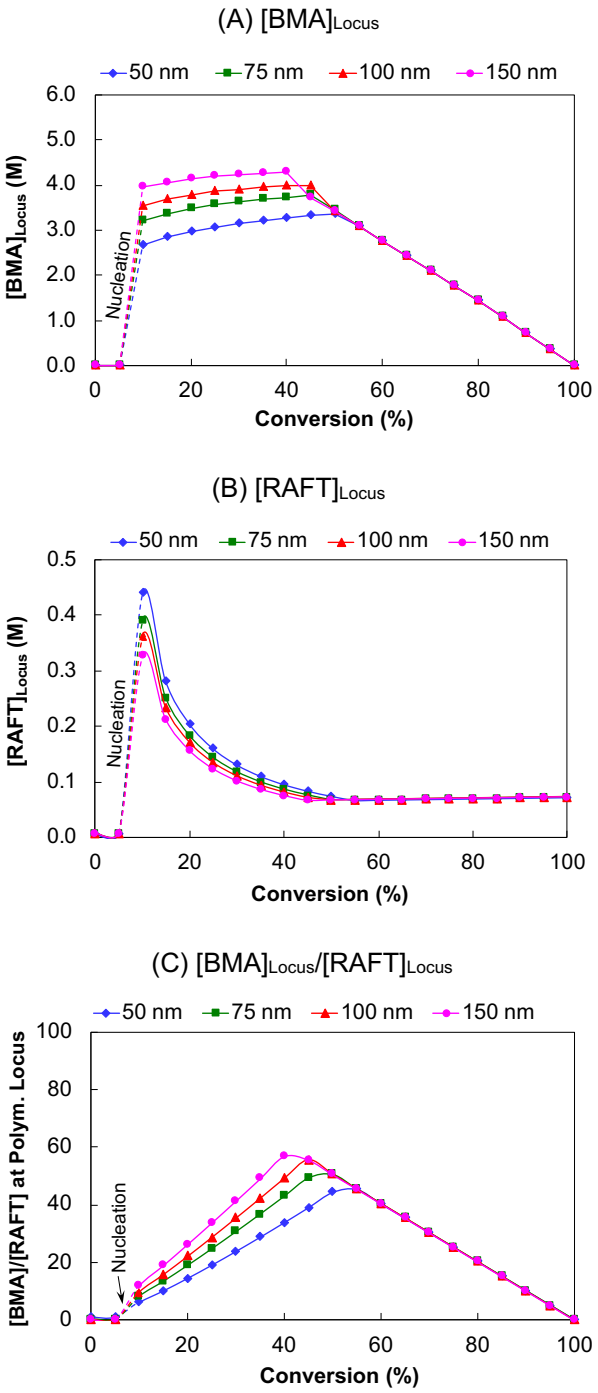

Figure 6 – Calculated values of [BMA] (A), [RAFT] (B) and [BMA]/[RAFT] (C) at the polymerization locus: effect of particle/droplet size. The detailed description of these calculations is presented in SI.

Methacrylate Chain Extensions and Multiblocks in RAFT emulsion

The excellent control obtained from *ab initio* emulsion polymerization was then exploited to generate methacrylate diblock and multiblock copolymers. The $PBMA_{100}$ block prepared above (EP2, Table 1) was chain extended *in situ* with MMA (DP100) as a seeded emulsion polymerization. For comparison, the

PMMA$_{100}$ block (EP3; Table 1) was also extended with BMA (DP100); both polymerizations were taken to completion (99% monomer conversion; Table 2). For both chain extensions, additional initiator, equal in amount to that which had been consumed during generation of the first block, was added along with the monomer of choice. The resulting MWDs are shown in Figure 7.

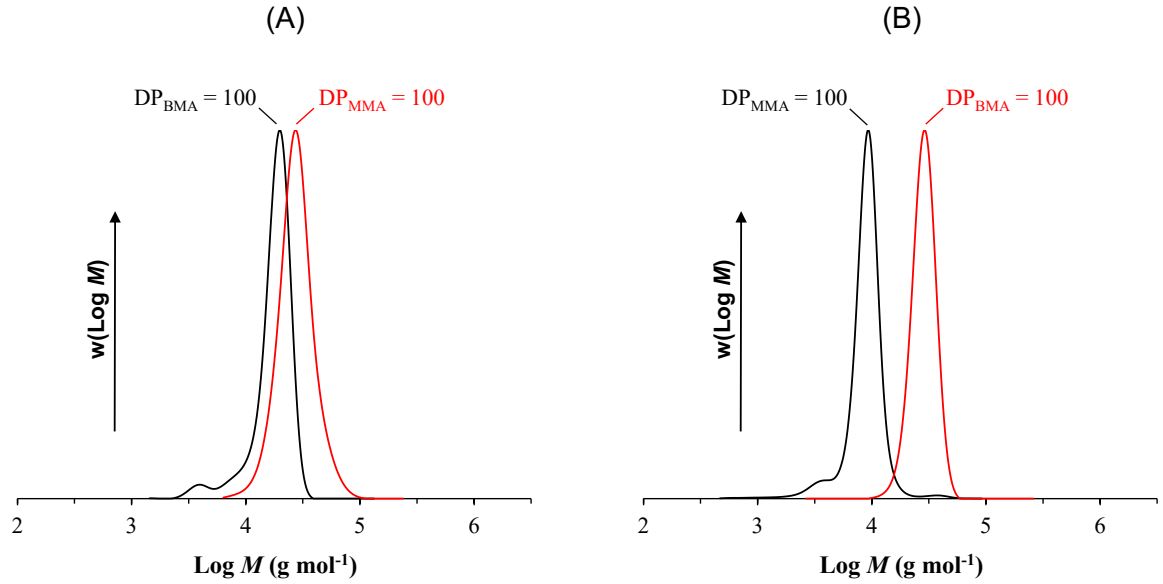

Figure 7: Molecular weight distribution overlays showing poly(BMA$_{100}$–*b*–MMA$_{100}$) (A) and poly(MMA$_{100}$–*b*–BMA$_{100}$) (B) (entries DP1/2 and DP3/4 in Table 2, respectively).

The final M_n for both diblocks was 28,500 PMMA equivalents and both the starting and final blocks have low dispersity ($Đ$ < 1.15) indicating that the chain extensions are controlled. It is noteworthy that the low MW shoulders present in the MWDs of both first blocks are not visible after chain extension, consistent with these low MW shoulders comprising unreacted initial PEG-ester CTA.

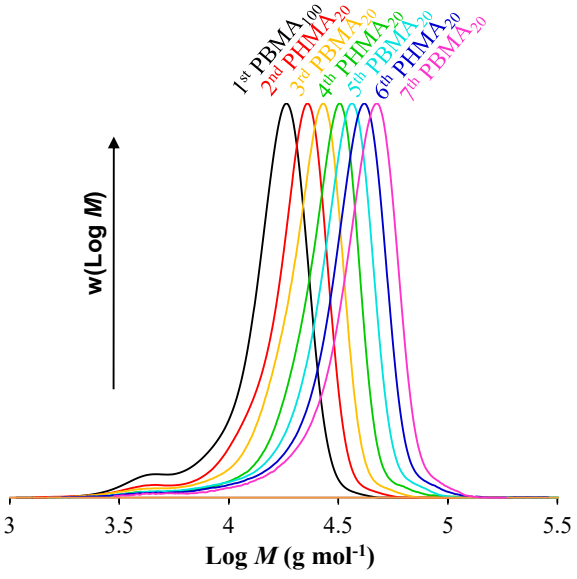

Figure 8: MWDs of BMA-HMA alternating multiblock copolymer (as detailed in Table 2).

To further illustrate the versatility of the system, the synthesis of a multiblock copolymer was subsequently attempted. The target heptablock, $PBMA_{100}$-*b*-$((PBMA_{20}$-*b*-$(PHMA_{20}))_3$, features a large first block to ensure maximal consumption of the initial PEG-ester CTA, followed by several smaller blocks. Initiator stock solution was added along with the next monomer for each block to replenish what had already decomposed. The GPC traces show that sequential addition of monomer leads to a regular increase in MW, indicating successful extension (Figure 8). For later blocks, tailing from shorter dead chains begins to broaden the dispersity, however, it remains below 1.20 for all blocks. As complete conversion of monomer had been shown to occur within 90 min, each block was simply produced by the addition of extra monomer without intermittent polymer purification.

Table 2 – Experimental conditions and results for RAFT polymerizations of various monomers yielding diblock copolymers and a multiblock copolymers employing seeded emulsion polymerizations.

Exp.	Mon	DP	[RAFT]/ [I]	X (%)/ t (h)	$M_{n,th}$ (g mol^{-1})	$M_{n,exp}$ (g mol^{-1})	$Đ$	Z_{av} *(nm) / PDI*
Diblock Synthesis								
DP1	BMA	100	8	99/1.5	16,520	16,000	1.09	75/0.03
DP2	BMA-MMA	100	8	99/1.5	26,468	28,500	1.15	163/0.09
DP3	MMA	100	8	99/1.5	12,312	9,000	1.10	60/0.39
DP4	MMA-BMA	100	8	99/1.5	26,468	28,500	1.13	174/0.44
Multiblock Synthesis								
MP1	BMA	100	8	99/1.5	16,520	16,500	1.07	76/0.01
MP2	HMA	20	8	99/1.5	19,360	19,500	1.07	91/0.01
MP3	BMA	20	8	99/1.5	22,760	22,000	1.09	128/0.01
MP4	HMA	20	8	99/1.5	25,600	25,500	1.13	159/0.03
MP5	BMA	20	8	99/1.5	29,000	28,000	1.14	190/0.05
MP6	HMA	20	8	99/1.5	31,840	30,500	1.17	216/0.09
MP7	**BMA**	**20**	**8**	**99/1.5**	**35,240**	**34,000**	**1.18**	**240/0.10**

Conclusions

We have demonstrate that the in-built monomer feeding mechanism in an emulsion polymerization can be used to dramatically increase RAFT control ($Đ \leq 1.15$) over methacrylate polymerization. An amphiphilic RAFT agent, based on a hydrophilic methacrylic R group and hydrophobic Z group, was used to mediate the polymerization of a range of methacrylate derivatives in heterogeneous and homogeneous systems. The miniemulsion and solution polymerizations were as anticipated observed to not be under RAFT control, a behaviour attributed to the low chain transfer constant ($C_{tr} \approx 11$) of the RAFT agent for methacrylates when functionalised with an R group generating tertiary radicals ($\cdot\mathbf{C}(CH_3)_2\text{-}COO\text{-}CH_2\text{-}CH_3$). The issue of a low C_{tr} was however overcome in emulsion polymerization by exploiting the fact that the ratio monomer / RAFT agent at the polymerization locus is lower than the overall ratio across the entire system due to the presence of monomer droplets. The mechanism of the polymerization was characterised with a theoretical model describing the monomer swelling of polymer particles. Exploiting this feature of emulsion polymerization, successive chain extension using PBMA polymer particles as seed latex enabled successful preparation of heptablock copolymer of high molecular weight and low dispersity (34,000 PMMA equivalents/ 1.18). Overall this work not only provides a deeper understanding of RAFT emulsion polymerization, but also demonstrates how emulsion polymerization can be successfully exploited for the preparation of multiblock copolymers.

References

1. Caldwell, R. B.; Toque, H. A.; Narayanan, S. P.; Caldwell, R. W., Arginase: an old enzyme with new tricks. *Trends in Pharmacological Sciences* **2015,** *36* (6), 395-405.
2. Sun, N.; Liu, M.; Wang, J.; Wang, Z.; Li, X.; Jiang, B.; Pei, R., Chitosan Nanofibers for Specific Capture and Nondestructive Release of CTCs Assisted by pCBMA Brushes. *Small* **2016,** *12* (36), 5090-5097.
3. Teulé, F.; Cooper, A. R.; Furin, W. A.; Bittencourt, D.; Rech, E. L.; Brooks, A.; Lewis, R. V., A protocol for the production of recombinant spider silk-like proteins for artificial fiber spinning. *Nature Protocols* **2009,** *4*, 341.
4. Baier, M.; Ruppertz, J. L.; Pfleiderer, M. M.; Blaum, B. S.; Hartmann, L., Synthesis of highly controlled carbohydrate–polymer based hybrid structures by combining heparin fragments and sialic acid derivatives, and solid phase polymer synthesis. *Chemical Communications* **2018,** *54* (74), 10487-10490.
5. Barnes, J. C.; Ehrlich, D. J. C.; Gao, A. X.; Leibfarth, F. A.; Jiang, Y.; Zhou, E.; Jamison, T. F.; Johnson, J. A., Iterative exponential growth of stereo- and sequence-controlled polymers. *Nature Chemistry* **2015,** *7*, 810.
6. Lutz, J. F.; Ouchi, M.; Liu, D. R.; Sawamoto, M., Sequence-Controlled Polymers. *Science* **2013,** *341* (6146), 628-+.
7. De Neve, J.; Haven, J. J.; Maes, L.; Junkers, T., Sequence-definition from controlled polymerization: the next generation of materials. *Polymer Chemistry* **2018,** *9* (38), 4692-4705.
8. Fu, C.; Huang, Z.; Hawker, C. J.; Moad, G.; Xu, J.; Boyer, C., RAFT-mediated, visible light-initiated single unit monomer insertion and its application in the synthesis of sequence-defined polymers. *Polymer Chemistry* **2017,** *8* (32), 4637-4643.

9. Soeriyadi, A. H.; Boyer, C.; Nystrom, F.; Zetterlund, P. B.; Whittaker, M. R., High-Order Multiblock Copolymers via Iterative Cu(0)-Mediated Radical Polymerizations (SET-LRP): Toward Biological Precision. *J. Am. Chem. Soc.* **2011,** *133* (29), 11128-11131.
10. Anastasaki, A.; Nikolaou, V.; Pappas, G. S.; Zhang, Q.; Wan, C.; Wilson, P.; Davis, T. P.; Whittaker, M. R.; Haddleton, D. M., Photoinduced sequence-control via one pot living radical polymerization of acrylates. *Chemical Science* **2014,** *5* (9), 3536-3542.
11. Anastasaki, A.; Nikolaou, V.; McCaul, N. W.; Simula, A.; Godfrey, J.; Waldron, C.; Wilson, P.; Kempe, K.; Haddleton, D. M., Photoinduced Synthesis of α,ω-Telechelic Sequence-Controlled Multiblock Copolymers. *Macromolecules* **2015,** *48* (5), 1404-1411.
12. Anastasaki, A.; Oschmann, B.; Willenbacher, J.; Melker, A.; Van Son, M. H. C.; Truong, N. P.; Schulze, M. W.; Discekici, E. H.; McGrath, A. J.; Davis, T. P.; Bates, C. M.; Hawker, C. J., One-Pot Synthesis of ABCDE Multiblock Copolymers with Hydrophobic, Hydrophilic, and Semi-Fluorinated Segments. *Angewandte Chemie International Edition* **2017,** *56* (46), 14483-14487.
13. Boyer, C.; Soeriyadi, A. H.; Zetterlund, P. B.; Whittaker, M. R., Synthesis of Complex Multiblock Copolymers via a Simple Iterative Cu(0)-Mediated Radical Polymerization Approach. *Macromolecules* **2011,** *44* (20), 8028-8033.
14. Boyer, C.; Derveaux, A.; Zetterlund, P. B.; Whittaker, M. R., Synthesis of multi-block copolymer stars using a simple iterative Cu(0)-mediated radical polymerization technique. *Polymer Chemistry* **2012,** *3* (1), 117-123.
15. Wenn, B.; Martens, A. C.; Chuang, Y. M.; Gruber, J.; Junkers, T., Efficient multiblock star polymer synthesis from photo-induced copper-mediated polymerization with up to 21 arms. *Polymer Chemistry* **2016,** *7* (15), 2720-2727.
16. Alsubaie, F.; Anastasaki, A.; Wilson, P.; Haddleton, D. M., Sequence-controlled multi-block copolymerization of acrylamides via aqueous SET-LRP at 0 °C. *Polymer Chemistry* **2015,** *6* (3), 406-417.
17. Gody, G.; Maschmeyer, T.; Zetterlund, P. B.; Perrier, S., Rapid and quantitative one-pot synthesis of sequence-controlled polymers by radical polymerization. *Nature Communications* **2013,** *4*, 2505.
18. Gody, G.; Maschmeyer, T.; Zetterlund, P. B.; Perrier, S., Rapid and quantitative one-pot synthesis of sequence-controlled polymers by radical polymerization. *Nature Communications* **2013,** *4*.
19. Gody, G.; Maschmeyer, T.; Zetterlund, P. B.; Perrier, S., Pushing the Limit of the RAFT Process: Multiblock Copolymers by One-Pot Rapid Multiple Chain Extensions at Full Monomer Conversion. *Macromolecules* **2014,** *47* (10), 3451-3460.
20. Gody, G.; Maschmeyer, T.; Zetterlund, P. B.; Perrier, S., Exploitation of the Degenerative Transfer Mechanism in RAFT Polymerization for Synthesis of Polymer of High Livingness at Full Monomer Conversion. *Macromolecules* **2014,** *47* (2), 639-649.
21. Zetterlund, P. B.; Gody, G.; Perrier, S., Sequence-Controlled Multiblock Copolymers via RAFT Polymerization: Modeling and Simulations. *Macromolecular Theory and Simulations* **2014,** *23* (5), 331-339.
22. Guimaraes, T. R.; Khan, M.; Kuchel, R. P.; Morrow, I. C.; Minami, H.; Moad, G.; Perrier, S.; Zetterlund, P. B., Nano-Engineered Multiblock Copolymer Nanoparticles via Reversible Addition-Fragmentation Chain Transfer Emulsion Polymerization. *Macromolecules* **2019,** *52* (8), 2965-2974.
23. Thickett, S. C.; Gilbert, R. G., Emulsion polymerization: State of the art in kinetics and mechanisms. *Polymer* **2007,** *48* (24), 6965-6991.
24. Zetterlund, P. B., Controlled/living radical polymerization in nanoreactors: compartmentalization effects. *Polym. Chem.* **2011,** *2* (3), 534-549.
25. Khan, M.; Guimarães, T. R.; Zhou, D.; Moad, G.; Perrier, S.; Zetterlund, P. B., Exploitation of Compartmentalization in RAFT Miniemulsion Polymerization to Increase the Degree of Livingness. *Journal of Polymer Science Part A: Polymer Chemistry* **2019,** *57* (18), 1938-1946.
26. Engelis, N. G.; Anastasaki, A.; Nurumbetov, G.; Truong, N. P.; Nikolaou, V.; Shegiwal, A.; Whittaker, M. R.; Davis, T. P.; Haddleton, D. M., Sequence-controlled methacrylic multiblock copolymers via sulfur-free RAFT emulsion polymerization. *Nature Chemistry* **2017,** *9* (2), 171-178.
27. Krstina, J.; Moad, G.; Rizzardo, E.; Winzor, C. L.; Berge, C. T.; Fryd, M., Narrow polydispersity block copolymers by free-radical polymerization in the presence of macromonomers. *Macromolecules* **1995,** *28* (15), 5381-5385.

28. Krstina, J.; Moad, C. L.; Moad, G.; Rizzardo, E.; Berge, C. T.; Fryd, M. In *A new form of controlled growth free radical polymerization*, Macromolecular Symposia, Wiley Online Library: 1996; pp 13-23.
29. Moad, G.; Chiefari, J.; Chong, Y. K.; Krstina, J.; Mayadunne, R. T. A.; Postma, A.; Rizzardo, E.; Thang, S. H., Living free radical polymerization with reversible addition–fragmentation chain transfer (the life of RAFT). *Polymer International* **2000,** *49* (9), 993-1001.
30. Moad, G.; Anderson, A. G.; Ercole, F.; Johnson, C. H. J.; Krstina, J.; Moad, C. L.; Rizzardo, E.; Spurling, T. H.; Thang, S. H., Controlled-Growth Free-Radical Polymerization of Methacrylate Esters: Reversible Chain Transfer versus Reversible Termination. In *Controlled Radical Polymerization*, American Chemical Society: 1998; Vol. 685, pp 332-360.
31. Ferguson, C. J.; Hughes, R. J.; Pham, B. T. T.; Hawkett, B. S.; Gilbert, R. G.; Serelis, A. K.; Such, C. H., Effective ab Initio Emulsion Polymerization under RAFT Control. *Macromolecules* **2002,** *35* (25), 9243-9245.
32. Gurnani, P.; Cook, A. B.; Richardson, R. A. E.; Perrier, S., A study on the preparation of alkyne functional nanoparticles via RAFT emulsion polymerisation. *Polymer Chemistry* **2019,** *10* (12), 1452-1459.
33. Canning, S. L.; Smith, G. N.; Armes, S. P., A Critical Appraisal of RAFT-Mediated Polymerization-Induced Self-Assembly. *Macromolecules* **2016,** *49* (6), 1985-2001.
34. D'Agosto, F.; Rieger, J.; Lansalot, M., RAFT-mediated polymerization-induced self-assembly. *Angewandte Chemie International Edition n/a* (n/a).
35. Clothier, G. K. K.; Guimarães, T. R.; Khan, M.; Moad, G.; Perrier, S.; Zetterlund, P. B., Exploitation of the Nanoreactor Concept for Efficient Synthesis of Multiblock Copolymers via MacroRAFT-Mediated Emulsion Polymerization. *ACS Macro Letters* **2019,** *8* (8), 989-995.
36. Stoffelbach, F.; Tibiletti, L.; Rieger, J.; Charleux, B., Surfactant-Free, Controlled/Living Radical Emulsion Polymerization in Batch Conditions Using a Low Molar Mass, Surface-Active Reversible Addition-Fragmentation Chain-Transfer (RAFT) Agent. *Macromolecules* **2008,** *41* (21), 7850-7856.
37. Rieger, J.; Stoffelbach, F.; Bui, C.; Alaimo, D.; Jérôme, C.; Charleux, B., Amphiphilic Poly(ethylene oxide) Macromolecular RAFT Agent as a Stabilizer and Control Agent in ab Initio Batch Emulsion Polymerization. *Macromolecules* **2008,** *41* (12), 4065-4068.
38. Rieger, J.; Osterwinter, G.; Bui, C.; Stoffelbach, F.; Charleux, B., Surfactant-Free Controlled/Living Radical Emulsion (Co)polymerization of n-Butyl Acrylate and Methyl Methacrylate via RAFT Using Amphiphilic Poly(ethylene oxide)-Based Trithiocarbonate Chain Transfer Agents. *Macromolecules* **2009,** *42* (15), 5518-5525.
39. Stuart, M. C. A.; van de Pas, J. C.; Engberts, J. B. F. N., The use of Nile Red to monitor the aggregation behavior in ternary surfactant–water–organic solvent systems. *Journal of Physical Organic Chemistry* **2005,** *18* (9), 929-934.
40. Dominguez, A.; Fernandez, A.; Gonzalez, N.; Iglesias, E.; Montenegro, L., Determination of Critical Micelle Concentration of Some Surfactants by Three Techniques. *Journal of Chemical Education* **1997,** *74* (10), 1227.
41. Patist, A.; Bhagwat, S. S.; Penfield, K. W.; Aikens, P.; Shah, D. O., On the measurement of critical micelle concentrations of pure and technical-grade nonionic surfactants. *Journal of Surfactants and Detergents* **2000,** *3* (1), 53-58.
42. Garnier, S.; Laschewsky, A., New Amphiphilic Diblock Copolymers: Surfactant Properties and Solubilization in Their Micelles. *Langmuir* **2006,** *22* (9), 4044-4053.
43. Creutz, S.; van Stam, J.; De Schryver, F. C.; Jérôme, R., Dynamics of Poly((dimethylamino)alkyl methacrylate-block-sodium methacrylate) Micelles. Influence of Hydrophobicity and Molecular Architecture on the Exchange Rate of Copolymer Molecules. *Macromolecules* **1998,** *31* (3), 681-689.
44. Ganeva, D. E.; Sprong, E.; de Bruyn, H.; Warr, G. G.; Such, C. H.; Hawkett, B. S., Particle Formation in ab Initio RAFT Mediated Emulsion Polymerization Systems. *Macromolecules* **2007,** *40* (17), 6181-6189.
45. Keddie, D. J.; Moad, G.; Rizzardo, E.; Thang, S. H., RAFT Agent Design and Synthesis. *Macromolecules* **2012,** *45* (13), 5321-5342.
46. Asua, J. M., Miniemulsion polymerization. *Progress in polymer science* **2002,** *27* (7), 1283-1346.

47. Dos Santos, A. M.; Le Bris, T.; Graillat, C.; D'Agosto, F.; Lansalot, M., Use of a poly (ethylene oxide) MacroRAFT agent as both a stabilizer and a control agent in styrene polymerization in aqueous dispersed system. *Macromolecules* **2009,** *42* (4), 946-956.
48. Zetterlund, P. B.; D'hooge, D. R., The Nanoreactor Concept: Kinetic Features of Compartmentalization in Dispersed Phase Polymerization. *Macromolecules* **2019,** *52* (21), 7963-7976.
49. Moad, G.; Rizzardo, E.; Thang, S. H., Radical addition–fragmentation chemistry in polymer synthesis. *Polymer* **2008,** *49* (5), 1079-1131.
50. Truong, N. P.; Dussert, M. V.; Whittaker, M. R.; Quinn, J. F.; Davis, T. P., Rapid synthesis of ultrahigh molecular weight and low polydispersity polystyrene diblock copolymers by RAFT-mediated emulsion polymerization. *Polymer Chemistry* **2015,** *6* (20), 3865-3874.
51. Daniel, J.-C.; Pichot, C., *Les latex synthétiques: élaboration, propriétés, applications*. Lavoisier: 2006.
52. Gilbert, R. G., *Emulsion polymerization: a mechanistic approach*. Academic Pr: 1995.
53. Bauer, W., Methacrylic Acid and Derivatives. In *Ullmann's Encyclopedia of Industrial Chemistry*, Wiley-VCH: Weinheim, 2011.
54. Pokorný, R.; Zubov, A.; Matuška, P.; Lueth, F.; Pauer, W.; Moritz, H.-U.; Kosek, J., Process model for styrene and n-butyl acrylate emulsion copolymerization in smart-scale tubular reactor. *Industrial & Engineering Chemistry Research* **2016,** *55* (2), 472-484.
55. Warson, H., Emulsion polymerization, a mechanistic approach. R. G. Gilbert. Academic Press, London, 1995. pp. xviii + 362, price £55.00. ISBN 0-12-283060-1. *Polymer International* **1996,** *41* (3), 352-352.
56. Morton, M.; Kaizerman, S.; Altier, M. W., Swelling of latex particles. *Journal of Colloid Science* **1954,** *9* (4), 300-312.
57. Goto, A.; Fukuda, T., Kinetics of living radical polymerization. *Progress in Polymer Science* **2004,** *29* (4), 329-385.
58. Engelis, N. G.; Anastasaki, A.; Whitfield, R.; Jones, G. R.; Liarou, E.; Nikolaou, V.; Nurumbetov, G.; Haddleton, D. M., Sequence-Controlled Methacrylic Multiblock Copolymers: Expanding the Scope of Sulfur-Free RAFT. *Macromolecules* **2018,** *51* (2), 336-342.
59. Pepels, M. P. F.; Holdsworth, C. I.; Pascual, S.; Monteiro, M. J., RAFT-Mediated Emulsion Polymerization of Styrene with Low Reactive Xanthate Agents: Microemulsion-like Behavior. *Macromolecules* **2010,** *43* (18), 7565-7576.
60. Smulders, W.; Gilbert, R. G.; Monteiro, M. J., A Kinetic Investigation of Seeded Emulsion Polymerization of Styrene Using Reversible Addition−Fragmentation Chain Transfer (RAFT) Agents with a Low Transfer Constant. *Macromolecules* **2003,** *36* (12), 4309-4318.
61. Zetterlund, P. B.; Kagawa, Y.; Okubo, M., Controlled/living radical polymerization in dispersed systems. *Chemical reviews* **2008,** *108* (9), 3747-94.